

The star cluster frequency throughout the Large Magellanic Cloud

Andrés E. Piatti*

Observatorio Astronómico, Universidad Nacional de Córdoba, Laprida 854, 5000, Córdoba, Argentina

16 October 2013

ABSTRACT

We address the issue about the variation of the star cluster frequency (CF) in the Large Magellanic Cloud (LMC) in terms of the cluster spatial distribution. We adopted the LMC regions traced by Harris & Zaritsky (2009) and used an updated version of the cluster database compiled by Baumgardt et al. (2013). The CFs were produced by taking into account an appropriate selection of age bins. Since the uncertainty in a cluster’s age can be large compared to the size of the age bins, we account for the fact that a cluster could actually reside in one of a few adjacent age bins. We confirm that there exist some variations of the LMC CFs in terms of their spatial distributions, although some caveats should be pointed out. 30 Doradus resulted to be the region with the highest relative frequency of youngest clusters, while the $\log(t) = 9-9.5$ (1-3 Gyr) age range is featured by cluster formation at a higher rate in the inner regions than in the outer ones. We compared the observed CFs to theoretical CFs, which are based on the star formation histories of the field stars in each region of the LMC, and found the former predicting more or fewer clusters than observed depending on the field and age range considered.

Key words: techniques: photometric – galaxies: individual: LMC – Magellanic Clouds – galaxies: star clusters.

* E-mail: andres@oac.uncor.edu

1 INTRODUCTION

The star cluster frequency (CF) - the number of clusters per time unit as a function of age - in the Large Magellanic Cloud (LMC) has been the subject of recent studies by Baumgardt et al. (2013, hereafter BPAG) and de Grijs et al. (2013, hereafter dGGA). Both works considered the LMC cluster population as a whole and produced overall CFs for the galaxy. BPAG showed that about 90% of all clusters older than 200 Myr are lost per dex of lifetime, which implies a cluster dissolution rate significantly faster than that based on analytic estimates and N-body simulations. However, dGGA showed that there is no evidence of significant destruction, other than that expected from stellar dynamics and evolution in simple population models for ages up to 1 Gyr ($\log(t)=9$).

On the other hand, different studies show that the LMC field star formation rate has varied from one place to another in the galaxy (Cole et al. 2005; Harris & Zaritsky 2009; Cioni et al. 2011; Rubele et al. 2011). Particularly, Harris & Zaritsky (hereafter HZ) concluded from the concordance between the star formation and chemical enrichment histories of the field and cluster populations that the field and cluster star formation modes are tightly coupled. Carrera et al. (2011) found that 10 different studied fields have age-metallicity relationships (AMRs) statistically distinguishable and that the disc AMR is similar to that of the clusters and is well reproduced by closed-box models or models with a small degree of outflow. Recently, Piatti & Geisler (2013) studied 21 LMC fields spread across the main body of the galaxy and found that the cluster and field AMRs show a satisfactory match only for the last 3 Gyr ($\log(t)=9.5$), while for the oldest ages (>11 Gyr ($\log(t)= 10.05$)) the cluster AMR is a remarkable lower envelope to the field AMR.

From these results, it would appear reasonable to infer that if the star formation history (SFH) of LMC field stars has been different throughout the galaxy, and field stars and clusters show some evidence of sharing the pace of their formation and chemical enrichment, then the CF should reflect the same spatial variation as seen in the field stars. However, as mentioned above, the LMC CF has been studied without making distinction on the cluster position. Thus, it is feasible that regions with a noticeable recent star formation activity were treated together with those more quiescent outer regions, and consequently the resultant CF pictured a mixed behaviour of the individual CFs. Here, we attempt to build CFs for different LMC regions taking advantage of those regions delimited by HZ and compare them to each other in order to find out some hints for any dependence of the CF with the position in the

galaxy. Fortunately, we have also the chance of comparing our results to the CFs coming from theoretical models computed from the SFHs recovered by HZ for different LMC regions.

The paper is organised as follows: Sect. 2 is devoted to describe the assembly of the available cluster age estimates into a robust compilation and to establish some procedures in order to properly deal with age bins and errors. Then, in Sect. 3 we discuss the level of completeness of the presently available cluster sample with age estimates and adopt some statistical rules for a reliable analysis of the resultant CFs, which is performed in Sect. 4 along with the comparison with theoretical CFs. Finally, Sect. 5 summarises the main conclusions.

2 HANDLING OF THE STAR CLUSTER SAMPLE

We are interested in building the CFs for clusters located in the HZ regions (see their Fig. 6), namely: the Bar, the Outer Bar, 30 Doradus, the Southeast Arm, the Northwest Arm, the Blue arm, Constellation III, and the Northwest Void. We realise that there are other parts of the LMC that could be meaningful from a particular astrophysical point of view. However, we prefer to use the HZ regions since they correspond to different galactic substructures where we can investigate CF variations. Furthermore, their available SFHs are useful to compute CFs from theoretical models as well. Recently, van der Marel & Kallivayalil (2013) showed that for most tracers (including clusters and field stars), the LMC's line-of-sight velocity dispersion is at least a factor ~ 2 smaller than their rotation velocity, which implies that the whole LMC is a kinematically cold disc system. Therefore, we assume that there probably has not been a statistically significant mixing of clusters from one region to another.

We used the catalogue of LMC clusters kindly provided by H. Baumgardt which contains ages, luminosities and masses for 1649 clusters (BPAG). We made an update of its ages and included more than 50% of the BPAG's intermediate-age clusters from our own catalogue of LMC clusters with ages and metallicities put into an homogeneous scale (Geisler et al. 1997; Bica et al. 1998; Piatti et al. 1999; Piatti et al. 2002; Geisler et al. 2003; Piatti et al. 2003a; Piatti et al. 2003b; Piatti et al. 2009; Piatti et al. 2011a; Piatti 2011; Piatti 2012; Piatti 2013; Palma et al. 2013), as well as all the clusters with ages estimated by Pietrzynski & Udalski (2000). We have paid attention to completing as much as possible of the sample of clusters older than 1 Gyr ($\log(t)=9$) since we are interesting in building CFs covering most of the galaxy lifetime. We do not focus on its youngest end, for which we refer to dGGA.

Fig. 1 depicts all the LMC clusters with age estimates represented by open circles. In the figure, we also included the LMC cluster candidates compiled in the general catalogue of extended objects by Bica et al. (2008, hereafter BBDS) represented by dots. Table 1 lists the number of clusters in the BBDS's catalogue with age estimates (open circles with central dots in fig. 1), as well as those with ages that were identified in later catalogues (taken from BPAG, open circles without central dots in Fig. 1). Notice that most of the clusters with age estimates have been included in the BBDS's compilation.

The first premise in building the CFs consisted in considering the age errors. Indeed, by taking into account such errors, the interpretation of the resultant CFs can differ appreciably from that obtained using only the measured ages without accounting for their uncertainties. However, the treatment of age errors in the CFs is not a straightforward task. Moreover, even if errors did not play an important role, the binning of age ranges could also bias the results. For instance, Bonatto et al. (2006) and Wu et al. (2009) used different fixed age intervals to build cluster age distributions using the same cluster database and found remarkably different results. At first glance, a fixed age bin size is not appropriate for yielding the intrinsic age distribution, since the result depends on the chosen age interval and the age errors are typically a strong function of the age. On the contrary, an age bin whose width is of the order of the age errors of the clusters in that interval appears to be more meaningful. This would lead to the selection of very narrow bins (in linear age) for young clusters and relatively broader age bins for the older ones.

Piatti (2010) took the uncertainties in the age estimates of Galactic open clusters into account in order to define the age intervals, with the aim of building an age histogram that best reproduces the intrinsic age distribution. Indeed, the age errors for very young clusters are a couple of Myrs, while those for the oldest clusters are at least a few Gyrs. Therefore, smaller bins are appropriate for young clusters, whereas larger bins are more suitable for the old clusters. In practice, he varied the bin size based on the average error of the age of the clusters that fall in each bin. Piatti et al. (2011a; 2011b) have also used these precepts for producing age distributions of clusters older than 1 Gyr ($\log(t)=9$) in both Magellanic Clouds.

In order to account for the effect of the age uncertainties in the CFs, we searched our list of LMC clusters and found that typical age errors are between $0.10 \lesssim \Delta \log(t) \lesssim 0.15$. Therefore, aiming at tracing the variation of the age uncertainties along the whole age range, we set the age bin sizes according to this logarithmic law to build CFs for the different HZ

regions. We used intervals of $\Delta\log(t) = 0.10$. At the same time, we focused on an additional issue. Even though the age bins are set to match the age errors, any individual point in the CF may fall in the respective age bin or in any of the two adjacent bins. This happens when an age point does not fall in the bin centre and, due to its errors, has the chance to fall outside it. Note that, since we chose bin dimensions as large as the involved errors, such points should not fall on average far beyond the adjacent bins. However, this does not necessarily happen to all age points, and we should consider at the same time any other possibility.

For our purposes, we first considered the cluster age range split in bins with sizes following the logarithmic law mentioned above. On the other hand, each age point with its error ($\sigma(age)$) covers a segment whose size is given by $2 \times \sigma(age)$, and may or may not fall centred on one of the age bins, and has dimensions smaller, similar or larger than the age bin wherein it is placed. These scenarios generate a variety of possibilities, in the sense that the age segment could cover from one up to 5 age bins depending on its position and size. For this reason, we weighed the contribution of each age point to each one of the age bins occupied by it, so that the sum of all the weights equals unity. The assigned weight was computed as the fraction of its age segment $[2 \times \sigma(age)]$ that falls in the age bin. In practice, we focused on a single age bin and computed the weighted contribution of all the age points to that age bin. Then we repeated the calculation for all the age bins. The challenge of knowing whether a portion of an age point (an age segment strictly speaking) falls in an age bin, was solved by taking into account the following possibilities of combination between them. For each age interval we looked for clusters with ages that fall inside the considered age bin, as well as clusters where age $\pm \sigma(age)$ could cause them to fall in the considered age bin. Note that if age $\pm \sigma(age)$ causes a cluster to step over the considered age bin (e.g. from one bin younger to one bin older), then we consider that that cluster may have an age that places it inside the considered age interval as well.

To illustrate how CF built with and without bin size and error effects differ, we plot in Fig. 2 the CF obtained by BPAG and that from our approach represented by filled circles and the solid line, respectively. Both CFs have been normalized to the total number of clusters.

3 COMPLETENESS OF THE STAR CLUSTER SAMPLE

BPAG and dGGA have imposed mass limits to their LMC cluster samples in order to deal with statistically complete lists. BPAG built the global LMC CF with 322 clusters older than 10^7 yrs, brighter than $M_V = -3.5$, and more massive than $5000 M_\odot$, from an original list of 1649 clusters. This means that they used the 322 clusters as representative of the LMC cluster population rather than the extended 1649 cluster sample. On the other hand, dGGA conducted different analyses by using a 50% completeness limit, $M_V = -4.3$ mag, based on single stellar population models. In this case, the minimum mass varies as a function of the age and the CF was consequently built from different cluster subsamples.

As a starting point, we also followed the recommendation of managing a statistically significant sample of clusters by applying some sort of selection. Since we basically used the mass values provided by H. Baumgardt for the BPAG cluster list, and those obtained by Piatti (2011) for the additional intermediate-age clusters of our own catalogs, we constrained the cluster sample to those with masses higher than $5 \times 10^3 M_\odot$ and $(1.8 \times \log(t) - 12.8) M_\odot$ for ages younger and older than 1 Gyr ($\log(t)=9$), respectively. The resultant CFs normalized to the total number of clusters used for each HZ region are shown in Fig. 3 with dashed lines. Notice that they account for bin size and age uncertainty effects, so that they show the main fiducial features of the LMC CFs.

Bearing in mind that we are interested in examining possible variations in the relative shape of the CFs in terms of the cluster position in the galaxy, some unavoidable questions arise: what is the benefit of using the above statistically complete sample instead of the whole available cluster sample? How meaningful are the results based on the statistical sample?, etc. In order to bring over an answer, we built CFs including all the available clusters in the different HZ regions. As for the statistically constrained sample, they are also corrected from bin size and age error effects and normalized to the total number of clusters used. Fig. 3 depict the resultant CFs with solid lines. As can be seen, the BPAG's global mass cut-off does not result in a satisfactory statistically representative sample of the cluster population in the different HZ regions.

In order to find a more appropriate mass cut-off for the individual HZ regions, we produced mass distributions using age intervals of $\Delta \log(t) = 0.2$, from $\log(t) = 7.0$ to 10.0 , and took the lower mass values of the full width at half maximum (mean mass - $\sigma(\text{mass})$) of those observed cluster mass distributions. The 84% more massive (encompassed in the [mean

mass - $\sigma(\text{mass})$, highest mass] interval) of the whole cluster sample reached in general masses lower than $10^3 M_{\odot}$ for ages younger than 1 Gyr ($\log(t)=9$). Then, we produced normalized CFs using this new limit (see Fig. 4.) The difference between normalized CFs based on the statistically limited sample and on the whole cluster sample is mostly negligible, with the exception of some excess in the latter of intermediate-age clusters and very young clusters in the Blue Arm and in the Northwest Void, respectively. From this result we conclude that this mass cut-off sample is statistically representative of the whole sample of clusters with age estimates. Furthermore, Table 1 shows the number of clusters used in the mass cut-off sample and the percentage that they represent respect to the total number of clusters with age estimates. As can be seen, such percentages range from 28% up to 63%, with an average of 47%. This means that nearly the 50% more massive of the whole cluster sample with age estimates mostly trace the overall behaviour of the CFs. Alternatively, clusters with masses below the mass cut-off limit do not contribute significantly to the normalized CFs, although they do represent on average nearly 50% of the total number of clusters with age estimates.

According to Fig. 1, the spatial distribution of catalogued clusters without age estimates (dots not encircled) does not seem to be particularly remarkable throughout the HZ regions. They are more or less distributed between those with age estimates (dots encircled and open circles) covering similar areas. One exception arises: the Southeast Arm. For the remaining HZ regions, the number of catalogued clusters without age estimate represent a relative minority respect to the total number of catalogued clusters as listed in Table 1 (column 5). In this context, we wonder whether the clusters without ages can be assumed to follow the same age distribution as the clusters with ages. We address this issue by assuming nine hypothetical different age distributions for the total number of clusters without age estimates. We cover scenarios from placing the clusters in the same age bin until distributing them uniformly along the age range $\log(t) = 7.0 - 9.0$. Then, we added these age distributions to those previously obtained for the different HZ regions, and computed the respective normalized CFs. The resultant CFs (see Appendix A for details) show that, for most of the HZ regions, clusters without ages could affect the CFs only if all of them fell in the youngest or in the oldest age bin ($\log(t) = 7.0$ or 9.0 , respectively). In the case of the Southeast Arm, any proposed scenario remarkably affects the CF.

An additional issue we would like to address is related to the completeness of the LMC cluster catalogue with respect to the whole LMC cluster population. The BBDS's catalogue include objects discovered by the *HST*, by the Optical Gravitational Lens Experiment

(OGLE) (Udalski 2003), etc. While the latter covers the central regions of the galaxy, the former only spots isolated small fields. On the other hand, the Magellanic Cloud Photometric Survey (MCPS) (Zaritsky et al. 2004) used by Glatt et al. (2010) to compile their own cluster database reaches a limiting magnitude between $V = 20$ and $V = 21$ mag, depending on the local degree of crowding in the images (Noël et al. 2009). According to dGGA, the depth of the observations made by OGLE is of the order 1.5 mag shallower than the MCPS. This means that the BBDS's catalogue is not as deep as that of Glatt et al. Indeed, some clusters with age estimates in the BPAG sample -who used the Glatt et al.'s compilation- are not included in the BBDS's catalogue (see open circles in Fig. 1). Nevertheless, since the derived CFs do not seem to show any arguable effect due to catalogued clusters without age estimates (except for the Southeast Arm), it might be also reasonable that our possible incompleteness of non-catalogued clusters (supposed to be fainter than the catalogued ones) do not play a role in the CFs either.

4 THE STAR CLUSTER FREQUENCIES

Fig. 5 depicts the resultant CFs from the statistically constrained cluster sample, corrected by bin size and age uncertainty effects. We have selected those objects which match the mass cut-off requirements mentioned above. Since all the CFs have been normalized to the total number of clusters employed, we did not need to shift them by any constant value for comparison purposes. Indeed, they are simply superimposed. From the figure, we confirm that there exist some variations of the LMC CF in terms of their spatial distributions, although some caveats should be pointed out. For instance, it seems that the period during which most of the CFs resemble each other occurred from $\log(t) \sim 8.0$ to 8.4 . However, more recently ($\log(t) < 7.5$) differential cluster formation rates have taken place, 30 Doradus being the region with the highest relative frequency of youngest star clusters in the galaxy. The Northwest Void presents the lowest CF during the last 30 Myr; the Outer Bar is at an intermediate level between 30 Doradus and the Northwest Void, while the Bar, the Southeast Arm, the Northeast Arm, and the Blue Arm have had a relatively lower cluster formation activity than the Outer Bar.

We also see interesting results in the $\log(t) \sim 9-9.5$ (1-3 Gyr) range, a period during which the Magellanic Clouds may have tidally interacted with each other (e.g. Diaz & Bekki 2011, Besla et al. 2012) and show an increase in the star formation rate of field stars (Weisz

et al. 2013). Besides the fact that this period of cluster formation is associated to bursting formation events after the enigmatic cluster age gap (Piatti 2011; Piatti & Geisler 2013), the resultant CFs show that such a formation period was more intense in the Bar, the Outer Bar, and the Northwest Arm; of an intermediate strength in 30 Doradus and the Northwest Void; while Constellation III, the Southeast Arm, and the Blue Arm account for the lowest cluster formation level. Focusing on the spatial distribution of these regions, the above result might be pointing out that the reservoirs of gas out of which the clusters were formed at that time were more important in the inner regions than in the outer ones, with some exception. Finally, the oldest LMC clusters located within the 8 HZ regions mainly populate the Bar, the Northwest Arm, and the Blue Arm. As is well-known, their origin is still a conundrum. While some authors suggest that they were formed during a very early and rapid period of enrichment (Piatti & Geisler 2013), others showed that some of those found in the outskirts of the LMC could have originally belonged to the Small Magellanic Cloud (Carpintero et al. 2013). Any way, our results witness that the oldest star clusters are not isotropically distributed.

Finally, we compared the present CFs to those obtained from theoretical models. The models were kindly provided by H. Baumgardt (personal communication). They assume that clusters are born with a power-law mass distribution with slope $\alpha = -2$ and with a rate that is proportional to the field star formation rate determined by HZ for each individual field, respectively, along with their corresponding uncertainties. The models then apply cluster dissolution due to stellar evolution, two-body relaxation and an external tidal field according to the EMACSS code (Alexander & Gieles 2012; Gieles et al. 2013). In addition, he used 300.000 clusters for each HZ region in order to have a good statistical sample. We applied mass cut-offs as described in Sect. 3 and normalized the theoretical CFs by the total number of clusters used, so that they can directly be compared to the observed ones. Fig. 6 shows the observed CFs (thin solid line) with the theoretical ones superimposed (thick gray solid line); the uncertainties in the latter being drawn with thick gray dotted lines. As can be seen, while the shapes of the theoretical CFs generally follow those of the observed CFs, the theoretical CFs vary between predicting more or fewer clusters than observed depending on the field and age range considered. If cluster dissolution were relatively well-known and easily modeled, then the above results would lead us to conclude that the LMC cluster population has not evolved as a coupled or independent system to the field star population,

exclusively, but as a combination of both scenarios that likely have varied in importance in different regions during the lifetime of the galaxy, with the coupled mode being dominating.

However, Lada & Lada (2003) suggested that most, if not all, stars form in some sort of cluster. This implies that field stars are the result of cluster dissolution and not from an independent formation mechanism. Based on their results, any difference between the observed and theoretical CFs would then be the result of different cluster dissolution rates as a function of mass and/or region. To this respect, there has been considerable debate about cluster dissolution rates and whether the rate is dependent on mass and environment, or if a certain percentage of clusters are destroyed each year regardless of any cluster or field properties (see, e.g., Bastian et al. 2011, and references therein). In this context, Fig. 6 would lead us to conclude that cluster dissolution rates are not universal, but instead may be affected by the masses of the clusters formed or the different environments in the LMC.

During the most recent star formation epoch ($\log(t) < 30$ Myr), the observed CFs in the Blue Arm, the Northwest Void, and possibly the Northwest Arm are lower than the corresponding counterparts in the theoretical scenario. However, there is a role reversal towards older ages until $\log(t) \sim 8.5$. On the contrary, the field star formation processes would seem to be relatively less significant than those for the clusters in the Bar and the Outer Bar during the last 30 Myrs. In the cases of the Outer Bar, 30 Doradus, and Constellation III such a trend keeps up until $\log(t) \sim 8.5$. As the $\log(t) = 9-9.5$ (1-3 Gyr) age range is concerned, the theoretical CFs obtained for the Blue Arm, Constellation III, Southeast Arm, and less importantly for the remaining HZ regions, appear to be higher than the observed ones. This behaviour might be originated by either a simple more active field star formation rate or by cluster dissolution or by both effects combined. Nevertheless, notice that for the outermost HZ regions not only the theoretical CFs (or indirectly the field star formation rates) are higher, but also the observed CFs are lower than those for the remaining HZ regions.

5 FINAL REMARKS

In this work we address for the first time the issue of the variation of the LMC CF in terms of the cluster spatial distribution. For this purpose, we adopted the LMC regions traced by HZ, namely: the Bar, the Outer Bar, 30 Doradus, the Southeast Arm, the Northwest Arm, the Blue arm, Constellation III, and the Northwest Void. As for the cluster database, we used

that of BPAG, which was updated by including more than 50% of their intermediate-age clusters as well as those from OGLE.

When building the CFs we took into account the influence of adopting arbitrary age bins, as well as the fact that each age value is associated to an uncertainty which allows the age value to fall centred on an age bin or outside it. We employed a procedure which achieves a compromise between the age bin size and the age errors. Particularly, we adopted an age bin size which varies with the age as a logarithmic law ($\Delta\log(t) = 0.1$). Then, we considered the possibility that the extension covered by an age value (properly a segment of $2\times\sigma(\text{age})$ long) may have a dimension smaller, similar or larger than the age bin wherein it is placed. The assigned weight was computed as the fraction of its age segment that falls in the age bin.

For each HZ region we produced mass distributions using age intervals of $\Delta\log(t) = 0.2$, from $\log(t) = 7.0$ to 10.0 , and took the lower mass values of the full width at half maximum (mean mass - $\sigma(\text{mass})$) of those observed cluster mass distributions. The 84% more massive of the whole cluster sample - encompassed in the (mean mass - $\sigma(\text{mass})$, highest mass) interval - reaches in general masses lower than $10^3 M_{\odot}$ for ages younger than 1 Gyr ($\log(t)=9$). In order to deal with a statistically significant cluster sample, we constrained the cluster sample to those with masses higher than $10^3 M_{\odot}$ and $(1.8\times\log(t) - 12.8) M_{\odot}$ for ages younger and older than 1 Gyr ($\log(t)=9$), respectively. Such mass cut-off sample includes from 28% up to 63%, with an average of 47%, of the more massive clusters in the whole cluster sample.

We confirm that there exist some variations of the LMC CFs in terms of their spatial distributions, although some caveats should be pointed out. For instance, it seems that the period during which most of the CFs resemble one to each other occurred from $\log(t) \sim 8.0$ to 8.4 . However, more recently ($\log(t) < 7.5$) differential cluster formation rates have taken place, 30 Doradus being the region with the highest relative frequency of young star clusters in the galaxy, while the Northwest Void presents the lowest CF during the last 30 Myr; the remaining HZ regions having intermediate levels of cluster formation activity. During the $\log(t)=9-9.5$ (1-3 Gyr) age range the resultant CFs show that the cluster formation proceeded more intensely in the inner regions than in the outer ones, while the oldest LMC clusters located within the 8 HZ regions mainly populate the Bar, the Northwest Arm, and the Blue Arm.

Finally, we compared the present CFs to those obtained from theoretical models assuming cluster formation rates similar to the star formation rates determined by HZ for their

individual LMC regions. We found that while the shapes of the theoretical CFs generally follow those of the observed CFs, the theoretical CFs vary between predicting more or fewer clusters than observed depending on the field and age range considered.

ACKNOWLEDGEMENTS

We are grateful for the comments and suggestions raised by the anonymous reviewer which helped us to improve the manuscript. We thank Holger Baumgardt for providing us with the theoretical models as well as with constructive suggestions. This work was partially supported by the Argentinian institution Agencia Nacional de Promoción Científica y Tecnológica (ANPCyT).

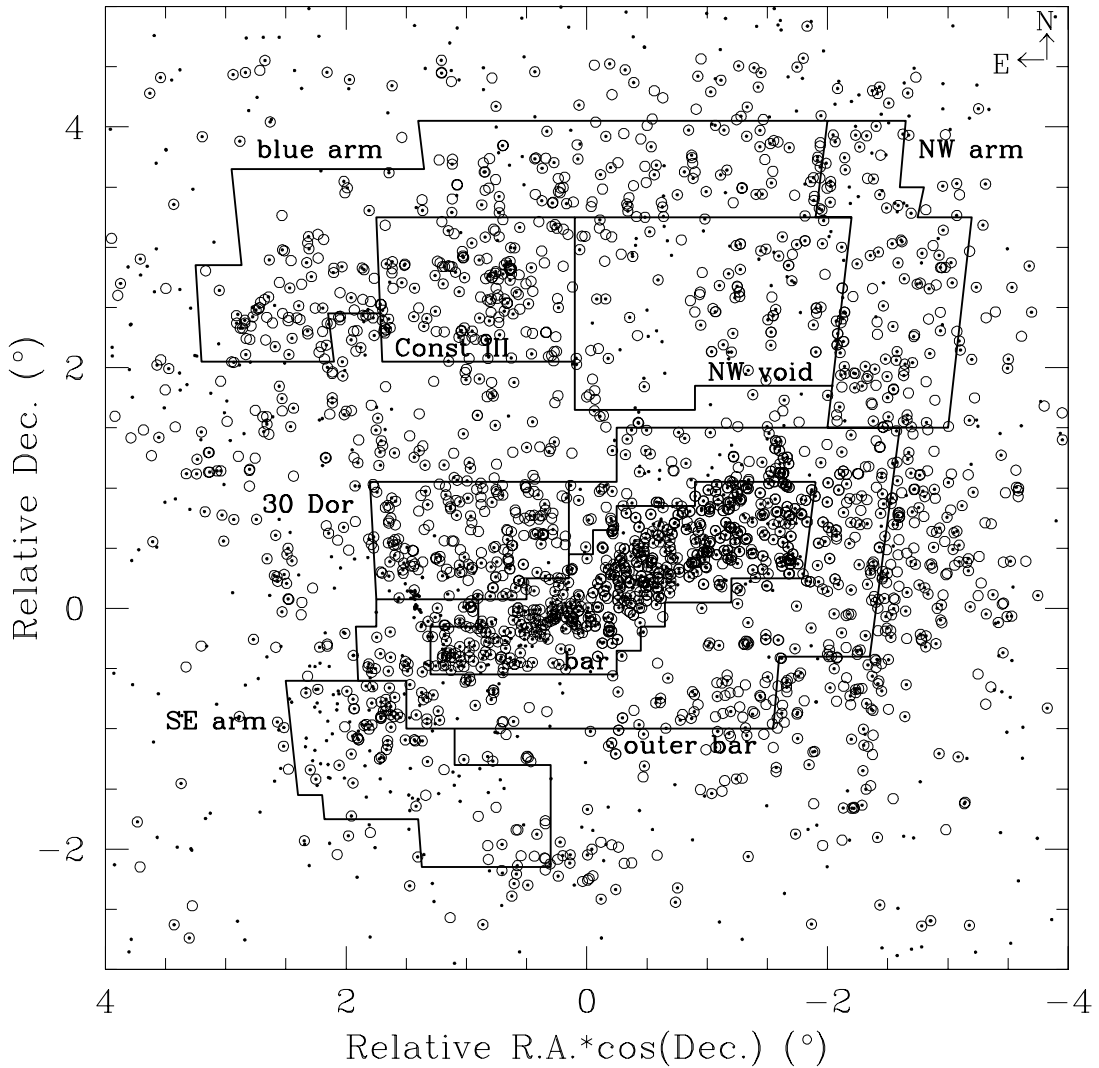
REFERENCES

- Alexander P., Gieles M., 2012, *MNRAS* 422, 3415
- Baumgardt H., Parmentier G., Anders P., Grebel E. K., 2013, *MNRAS*, 430, 676 (BPAG)
- Bastian N., Adamo A., Gieles M., Lamers H.J.G.L.M., Larsen S.S., Silva-Villa E., Smith L.J., Kotulla R., Konstantopoulos I.S., Trancho G., Zackrisson E., 2011, *MNRAS*, 417, L6
- Besla G., Kallivayalil N., Hernquist L., van der Marel R.P., Cox T.J., Kereš D., 2012, *MNRAS*, 421, 2109
- Bica E., Bonatto C., Dutra C.M., Santos Jr. J.F.C., 2008, *MNRAS*, 389, 678 (BBDS)
- Bica E., Geisler D., Dottori H., Piatti A.E., Clariá J.J., Santos Jr. J.F.C., 1998, *AJ*, 116, 723
- Bonatto C., Kerber L.O., Bica E., Santiago B.X., 2006, *A&A*, 446, 121
- Brocato E., Castellani V., Ferraro F.R., Piersimoni A.M., Testa V., 1996, *MNRAS*, 282, 614
- Carpintero, D.D., Gómez F.A., Piatti A.E., 2013, *MNRAS*, doi:10.1093/mnras/slt096
- Carrera R., Gallart C., Aparicio A., Hardy E., 2011, *AJ*, 162, 61
- Cioni M.R., Clementini G., Girardi L., Guandalini R., Gullieuszik M., Miszalski B., Moretti M.I., Ripepi V., et al., 2011, *A&A*, 527, 116
- Cole A.A., Tolstoy E., Gallagher J.S. III, Smecker-Hane T.A., 2005, *AJ*, 129, 1465 (Dordrecht : Kluwer),
- de Grijs R., Goodwin S.P., Anders P., 2013, *MNRAS*, (in press) (dGGA)
- Diaz J., Bekki K., 2011, *MNRAS*, 413, 2015
- Geisler D., Bica E., Dottori H., Clariá J.J., Piatti A.E., Santos Jr., J.F.C., 1997, *AJ*, 114, 1920
- Geisler D., Piatti A.E., Bica E., Clariá J.J. 2003, *MNRAS*, 341, 771
- Gieles M., Alexander P., Lamers H., Baumgardt H., 2013, *MNRAS* submitted
- Glatt K., Grebel E.K., Koch A., 2010, *A&A* 517, 50
- Harris J., Zaritsky D., 2009, *AJ*, 138, 1243 (HZ)
- Johnson J.A., Ivans I.I., Stetson P.B., 2006, *ApJ*, 640, 801
- Lada Ch.J., Lada E.A., 2003, *ARA&A*, 41, 57
- Mackey A.D., Gilmore G.F., 2004, *MNRAS*, 352, 153
- Marigo P., Girardi L., Bressan A., Groenewegen M.A.T., Silva L. Granato G.L., 2008, *A&A*, 482, 883
- Noël N.E.D., Aparicio A., Gallart C., Hidalgo S.L., Costa E., Méndez R.A., 2009, *ApJ*, 705, 1260
- Palma T., Clariá J.J., Geisler D., Piatti A.E., Ahumada A.V., 2013, *A&A*, 555, 131

- Piatti A.E., 2010, *A&A*, 513, L13
- Piatti A.E., 2011, *MNRAS*, 418, L40
- Piatti A.E., 2012, *A&A*, 540, A58
- Piatti A.E., 2013, *MNRAS*, 430, 2358
- Piatti A.E., Geisler D., 2013, *AJ*, 147, 17
- Piatti A.E., Bica E., Geisler D., Clariá J.J., 2003b, *MNRAS*, 344, 965
- Piatti A.E., Clariá J.J., Bica E., Geisler D., Ahumada A.V., Girardi L., 2011b, *MNRAS*, 417, 1559
- Piatti A.E., Clariá J.J., Parisi M.C., Ahumada A.V., 2011a, *PASP*, 123, 519
- Piatti A.E., Geisler D., Bica E., Clariá J.J., 2003a, *MNRAS*, 343, 851
- Piatti A.E., Geisler D., Bica E., Clariá J.J., Santos Jr. J.F.C., Sarajedini A., Dottori H., 1999, *AJ*, 118, 2865
- Piatti A.E., Geisler D., Sarajedini A., Gallart C., 2009, *A&A*, 501, 585
- Piatti A.E., Sarajedini A., Geisler D., Bica E., Clariá J.J., 2002, *MNRAS*, 329, 556
- Pietrzynski G., Udalski A., 2000, *Acta Astronomica*, 50, 337
- Rubele S., Kerber L., Girardi L. et al., 2011, *A&A*, 537, 106
- Udalski A., 2003, *Acta Astronomica*, 53, 291
- van der Marel R., Kallivayalil N., 2013, *ApJ*. (submitted, arXiv:1305.4641)
- Weisz D.R., Dolphin A.E., Skillman E.D., Holtzman J., Dalcanton J.J., Cole A.A., Neary K., 2013, *MNRAS*, 431, 364
- Wu Z.-Y., Zhou X., Ma J., Du C.-H., 2009, *MNRAS*, 399, 2146
- Zaritsky D., Harris J., Thompson I.B. et al., 2004, *AJ*, 128, 1606

Table 1. LMC cluster statistics.

HZ region	Clusters with age estimates		Clusters in the mass cut-off sample	Clusters without age estimates
	in BBDS	in other catalogs		
Bar	347	60	206 (51%)	52 (11%)
Outer Bar	168	43	114 (54%)	29 (12%)
30 Doradus	65	63	80 (63%)	19 (12%)
Southeast Arm	47	14	17 (28%)	50 (45%)
Northwest Arm	69	19	47 (54%)	17 (16%)
Blue Arm	84	63	73 (50%)	11 (7%)
Constellation III	60	55	53 (46%)	2 (2%)
Northwest Void	52	24	24 (32%)	25 (25%)

**Figure 1.** Spatial distribution of LMC clusters: those with an open circle have age estimates available. The clusters included in the BBDS's catalogue are represented by dots. The HZ regions are also overpotted.

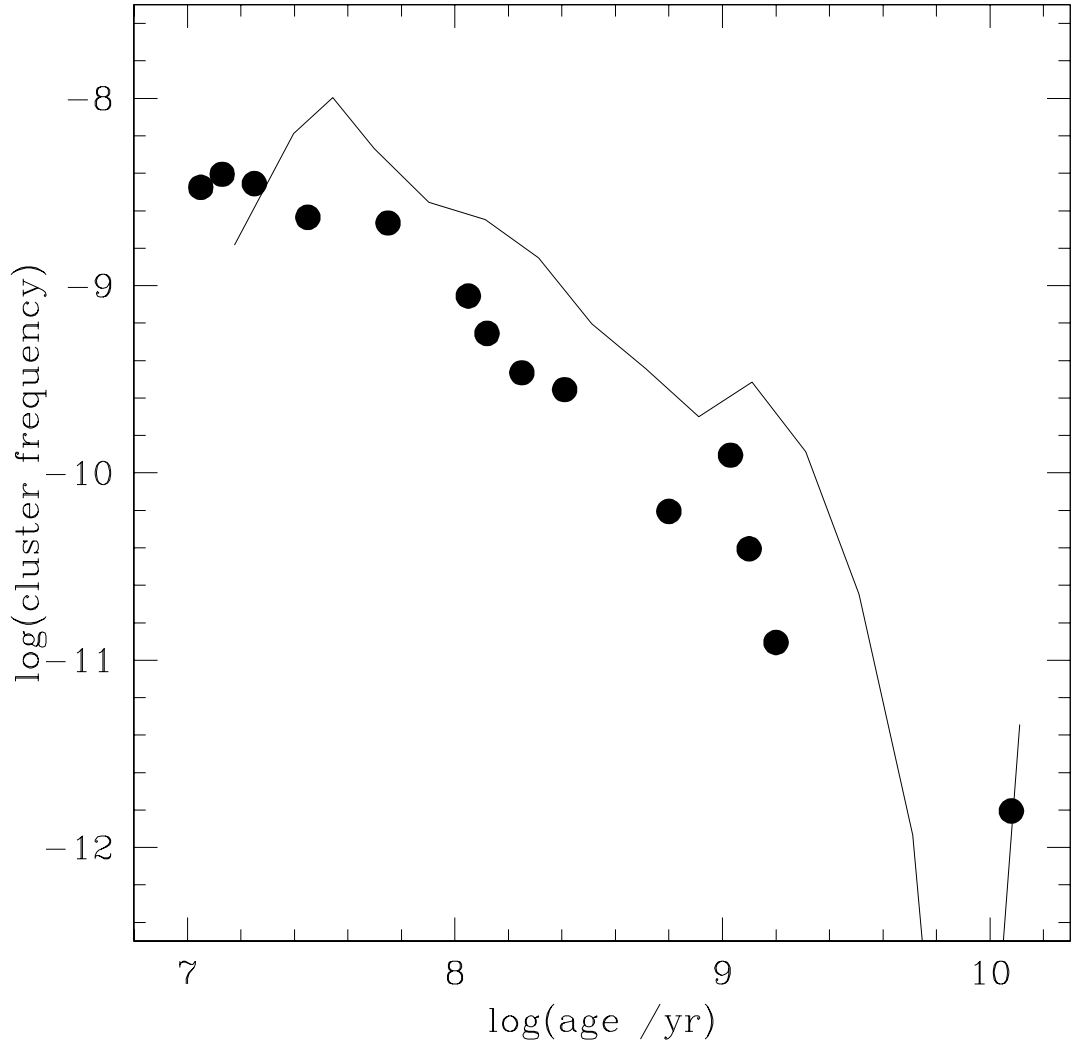


Figure 2. CFs obtained by BPAG and in the present work as described in Sect. 2 for the 322 BPAG's cluster sample, represented by filled circles and by a solid line, respectively. Both CFs have been normalized to the total number of clusters.

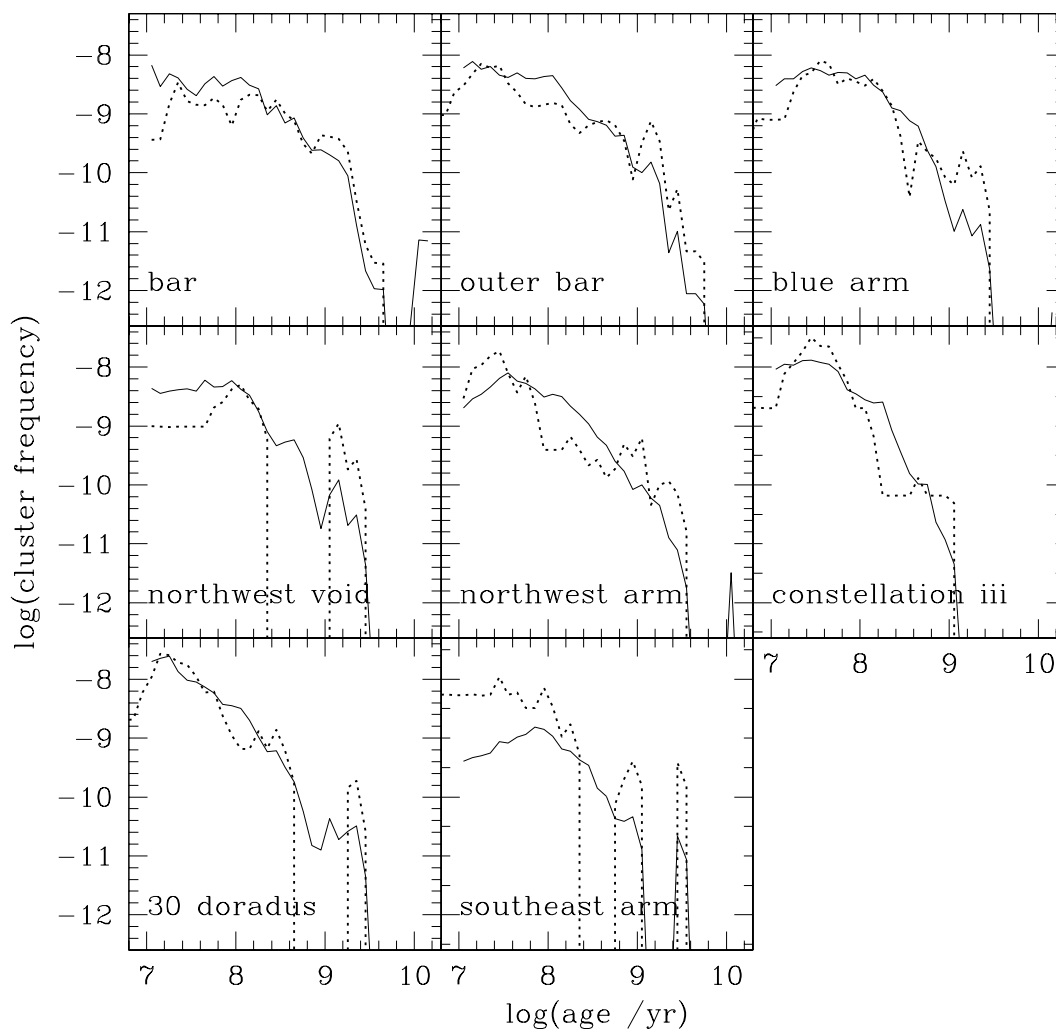


Figure 3. $5 \times 10^3 M_{\odot}$ cut-off CFs (dashed lines) compared to those built using the whole cluster sample (solid lines).

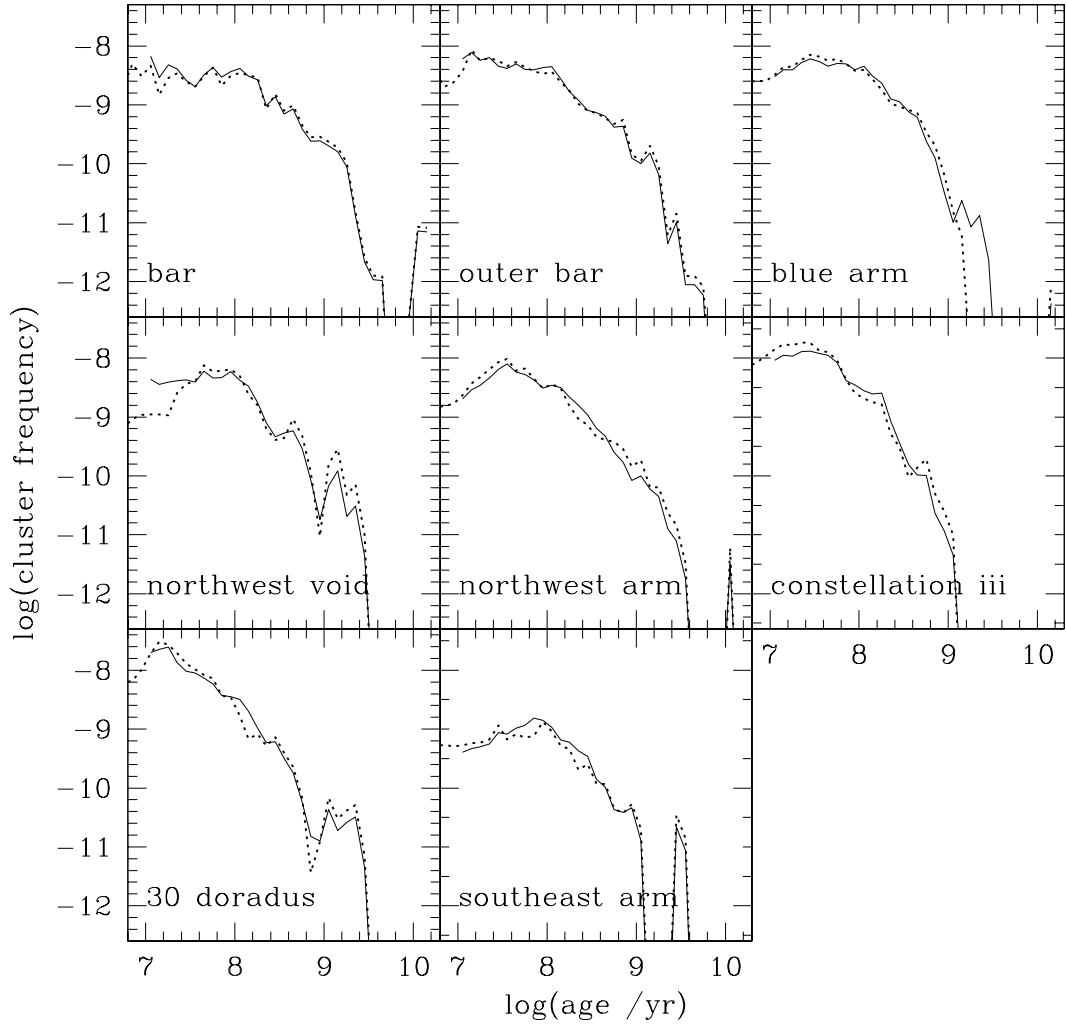


Figure 4. $10^3 M_{\odot}$ cut-off CFs (dashed lines) compared to those built using the whole cluster sample (solid lines).

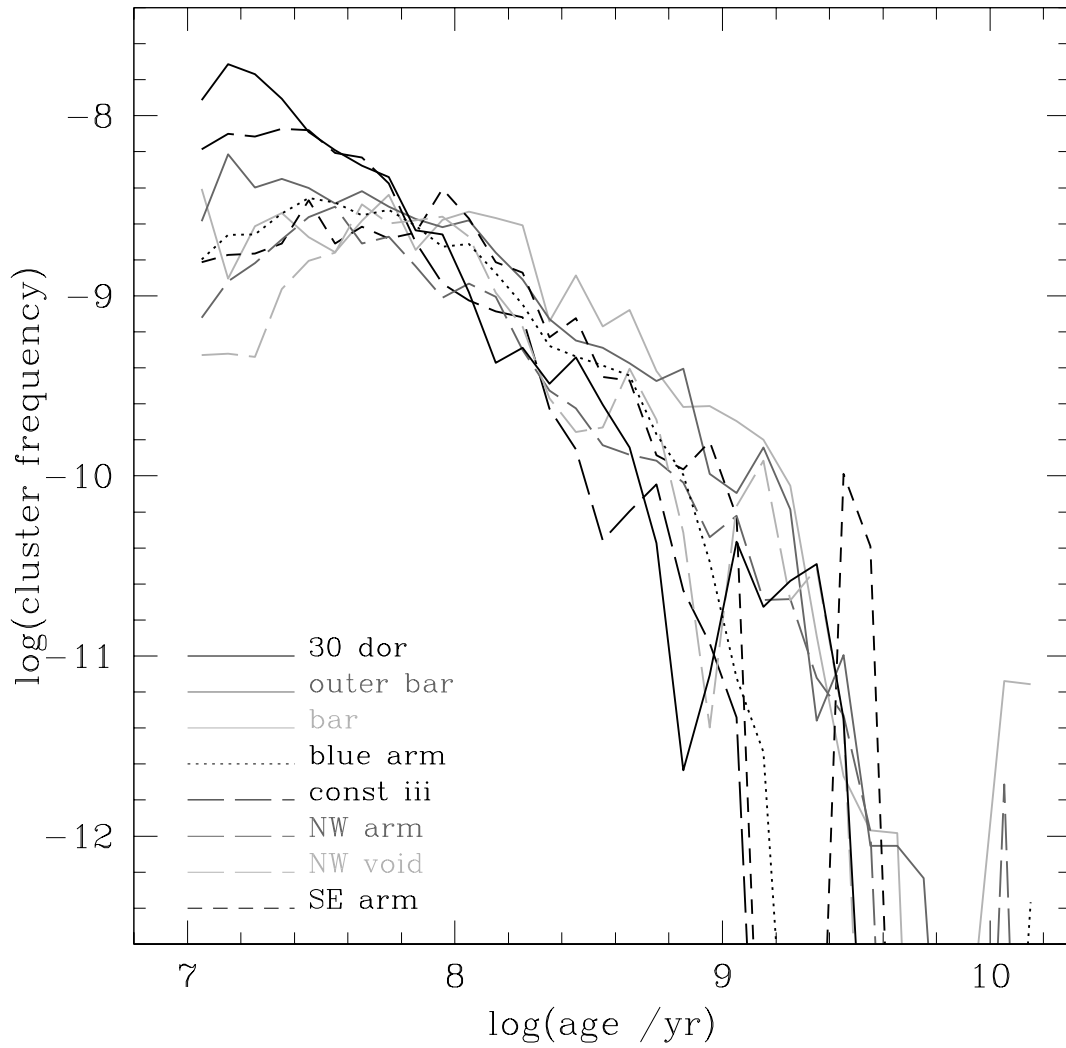


Figure 5. Mass cut-off CFs for different HZ regions.

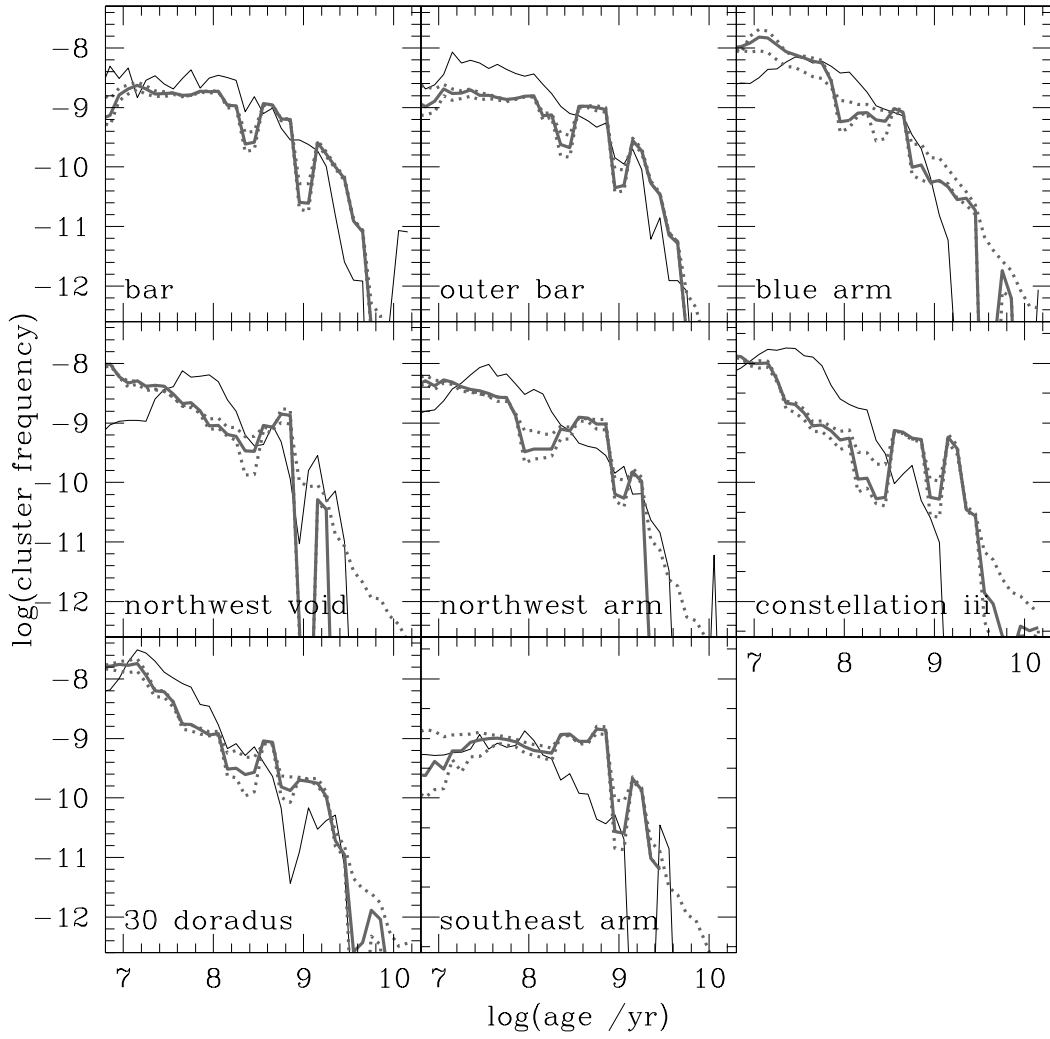


Figure 6. Comparison between the observed CFs (thin solid line) and the theoretical ones (thick gray solid line). The error curves for the latter are drawn with thick gray dotted lines.

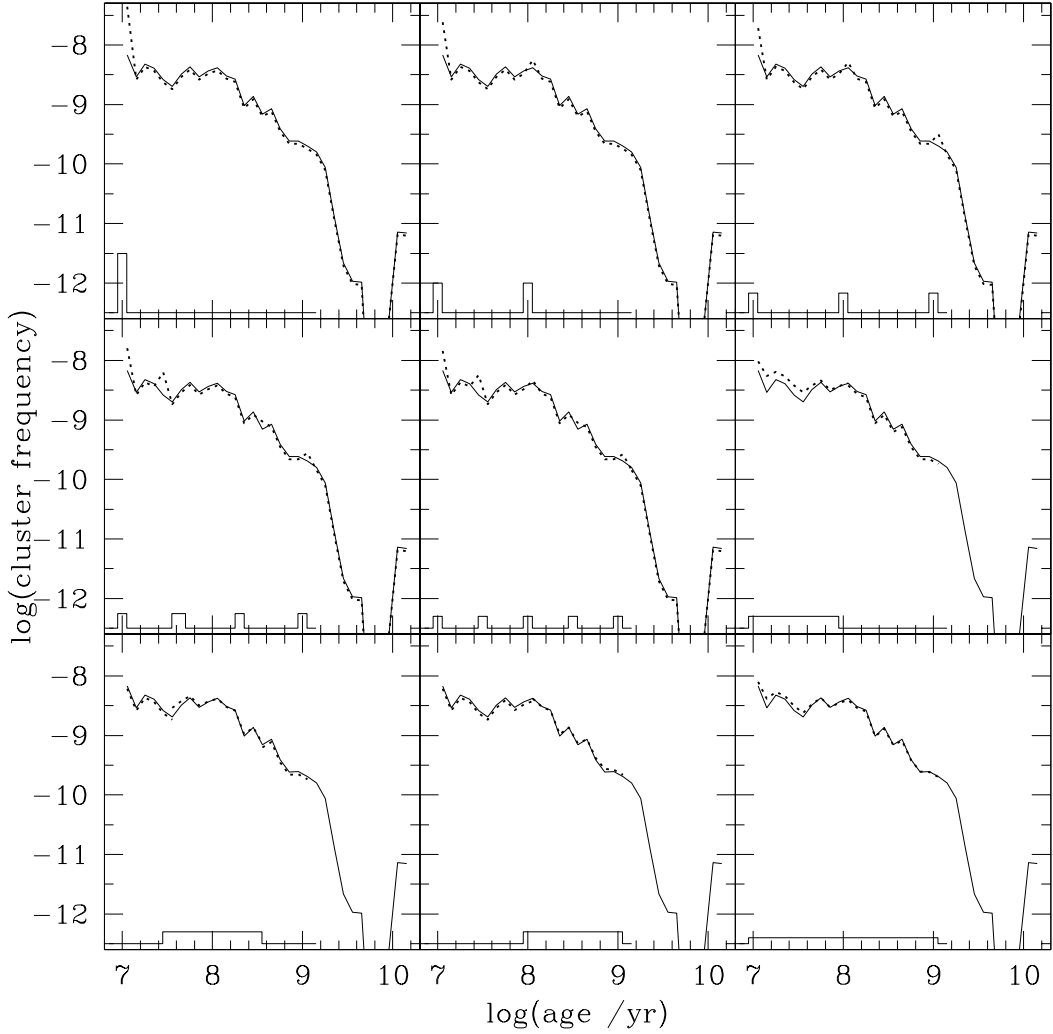


Figure A1. CFs for the LMC Bar (see Appendix A for details).

APPENDIX A: COMPLETENESS IN THE CLUSTER FREQUENCIES

We provide here with a series of experiments related to the effect that the clusters without age estimates might cause in the derived CFs (see Sect. 3). We produced multiple panel figures for the eighth HZ regions. Each panel shows the previously derived CF for the respective HZ region with a solid line, and the resultant CF according to different age distributions for the clusters without ages drawn with dotted lines. The employed normalized age distributions are included at the bottom of each panel.

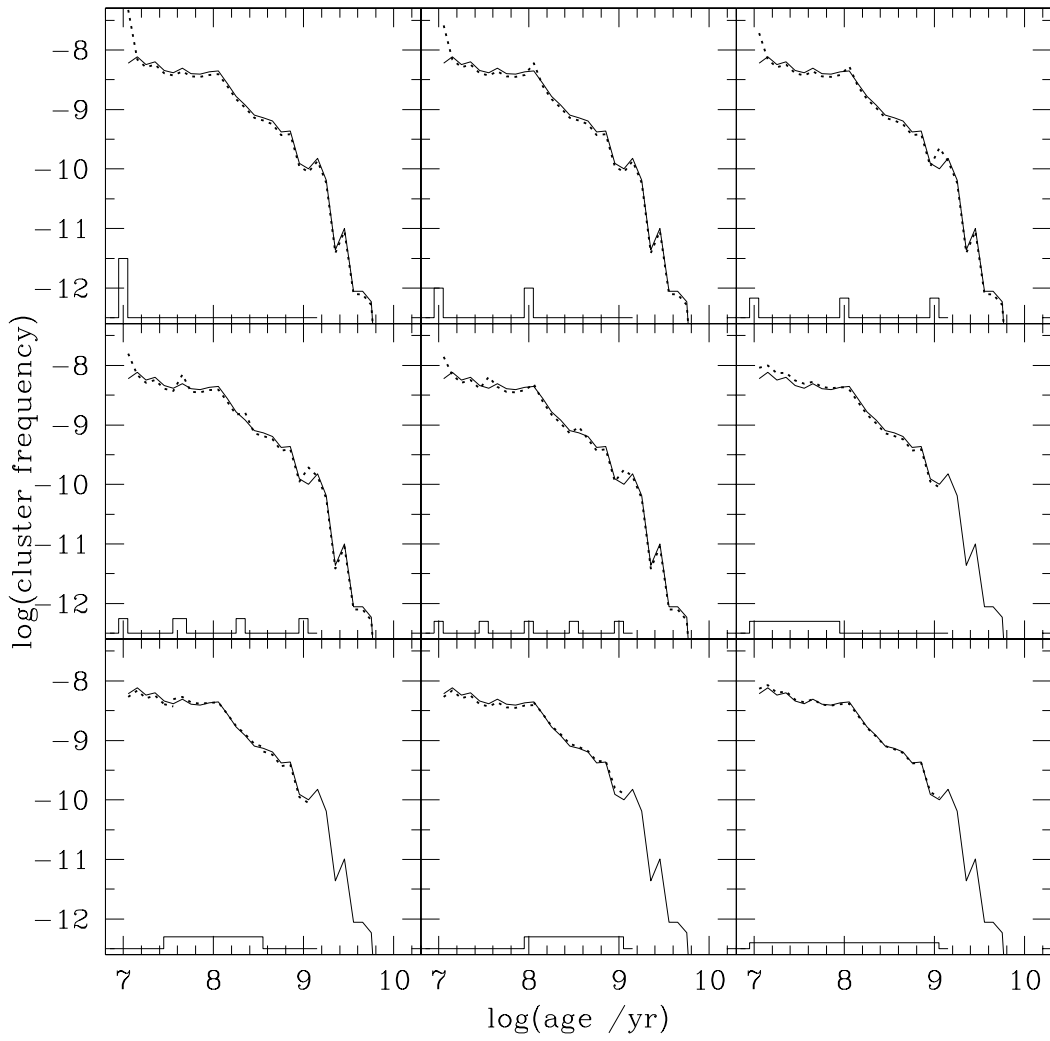


Figure A2. CFs for the LMC Outer Bar (see Appendix A for details).

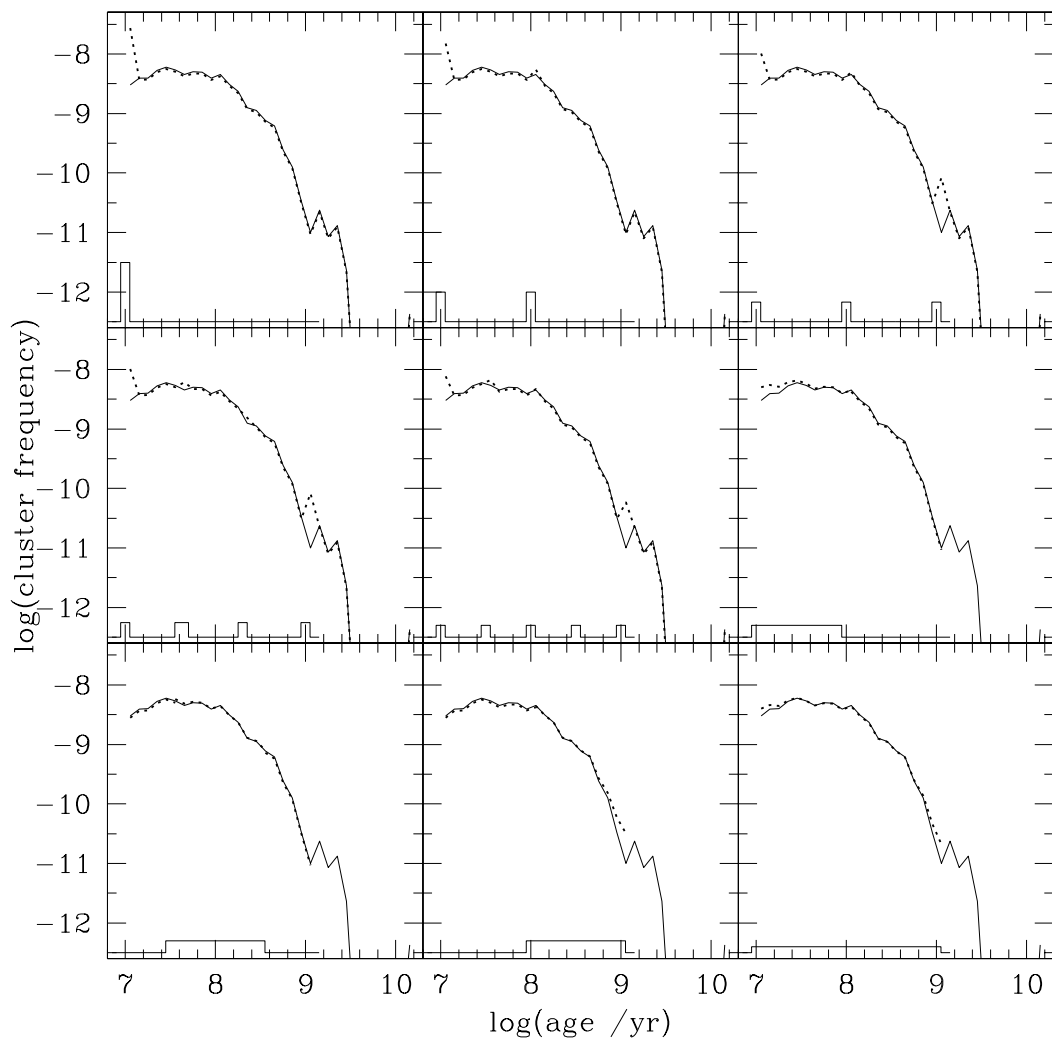


Figure A3. CFs for the LMC Blue Arm (see Appendix A for details).

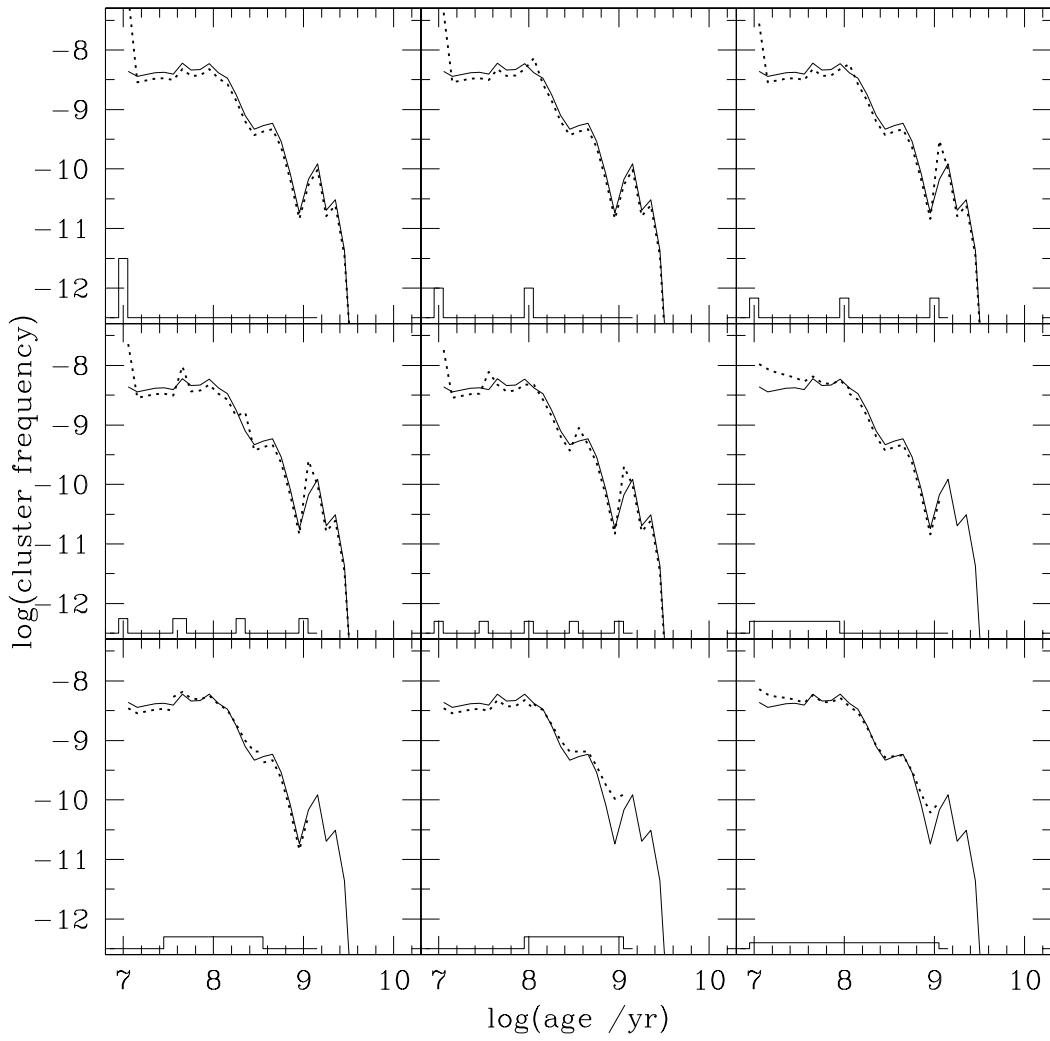


Figure A4. CFs for the LMC Northwest Void (see Appendix A for details).

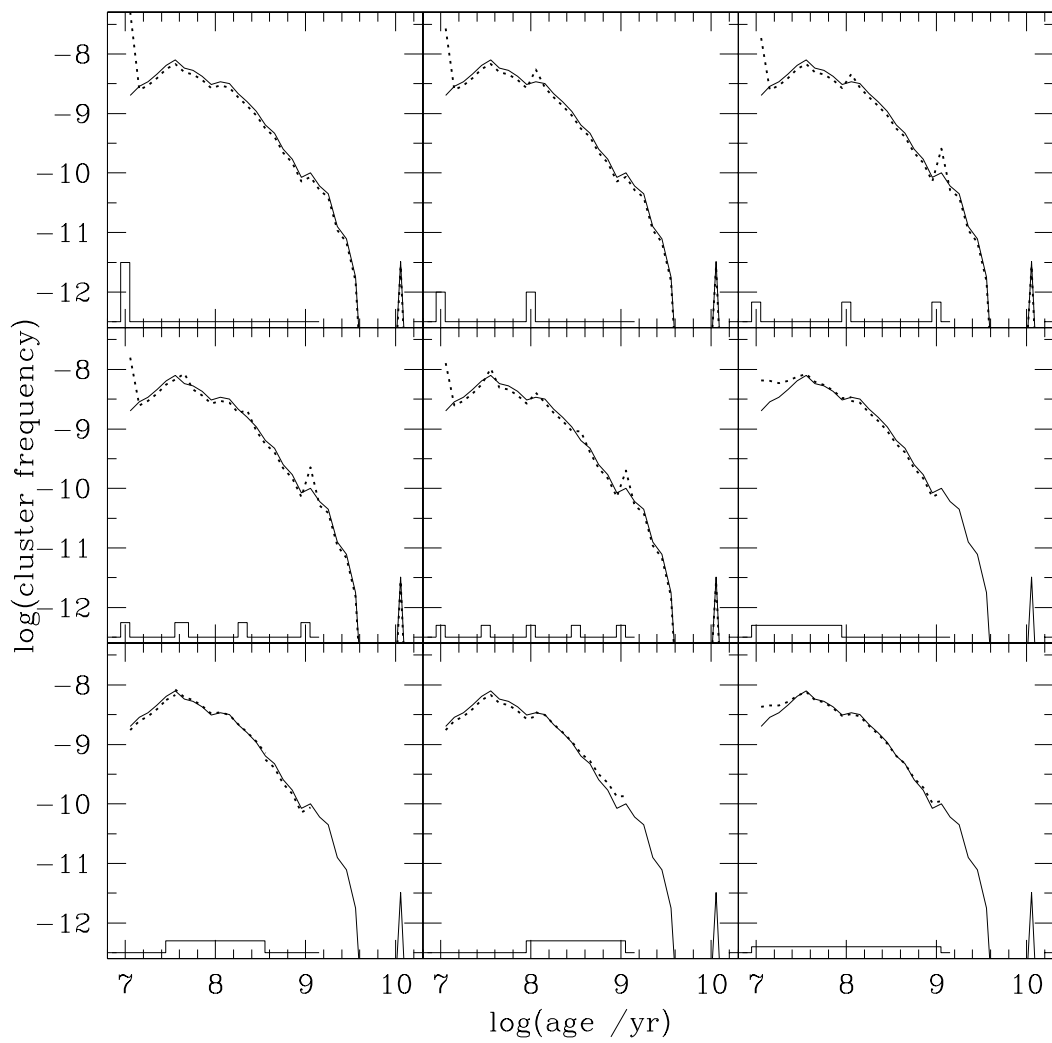


Figure A5. CFs for the LMC Northwest Arm (see Appendix A for details).

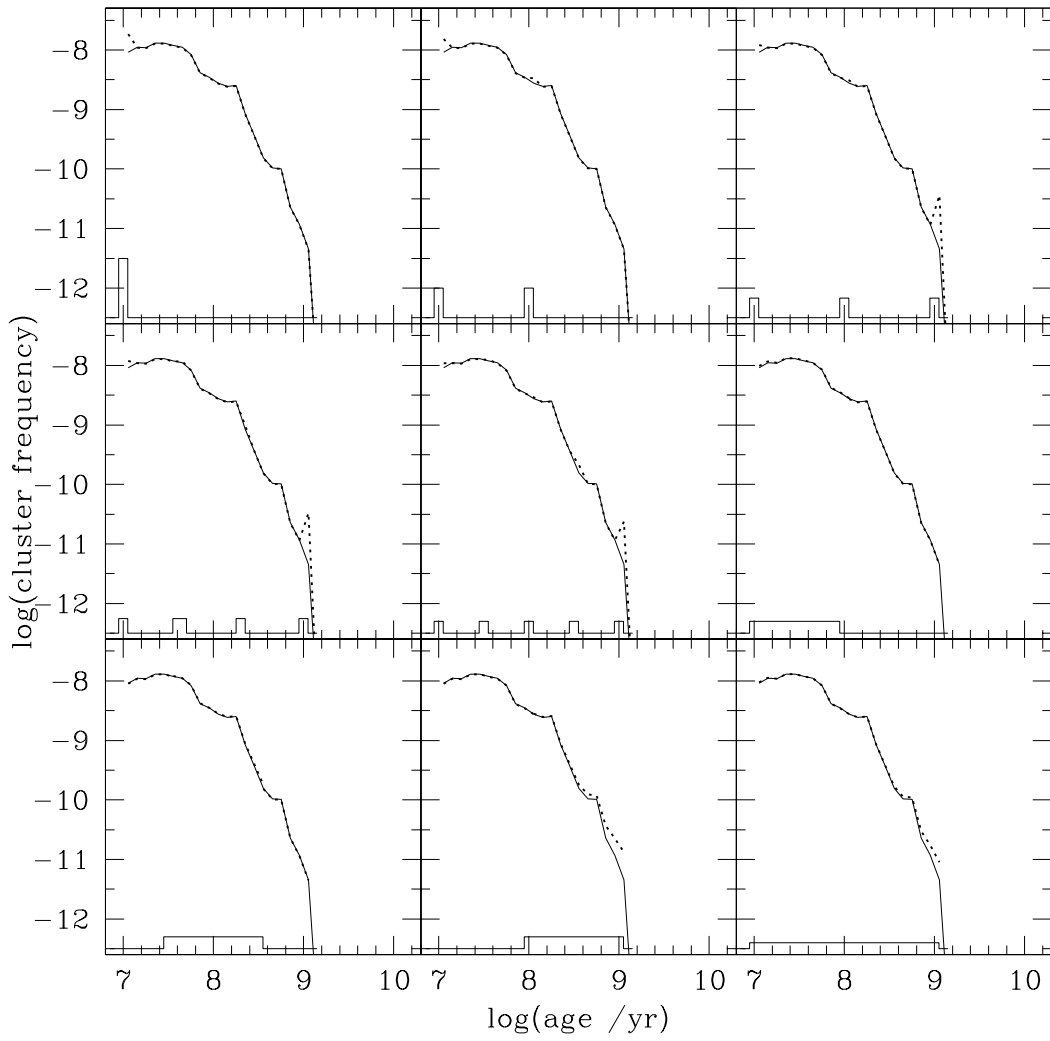


Figure A6. CFs for the LMC Constellation III (see Appendix A for details).

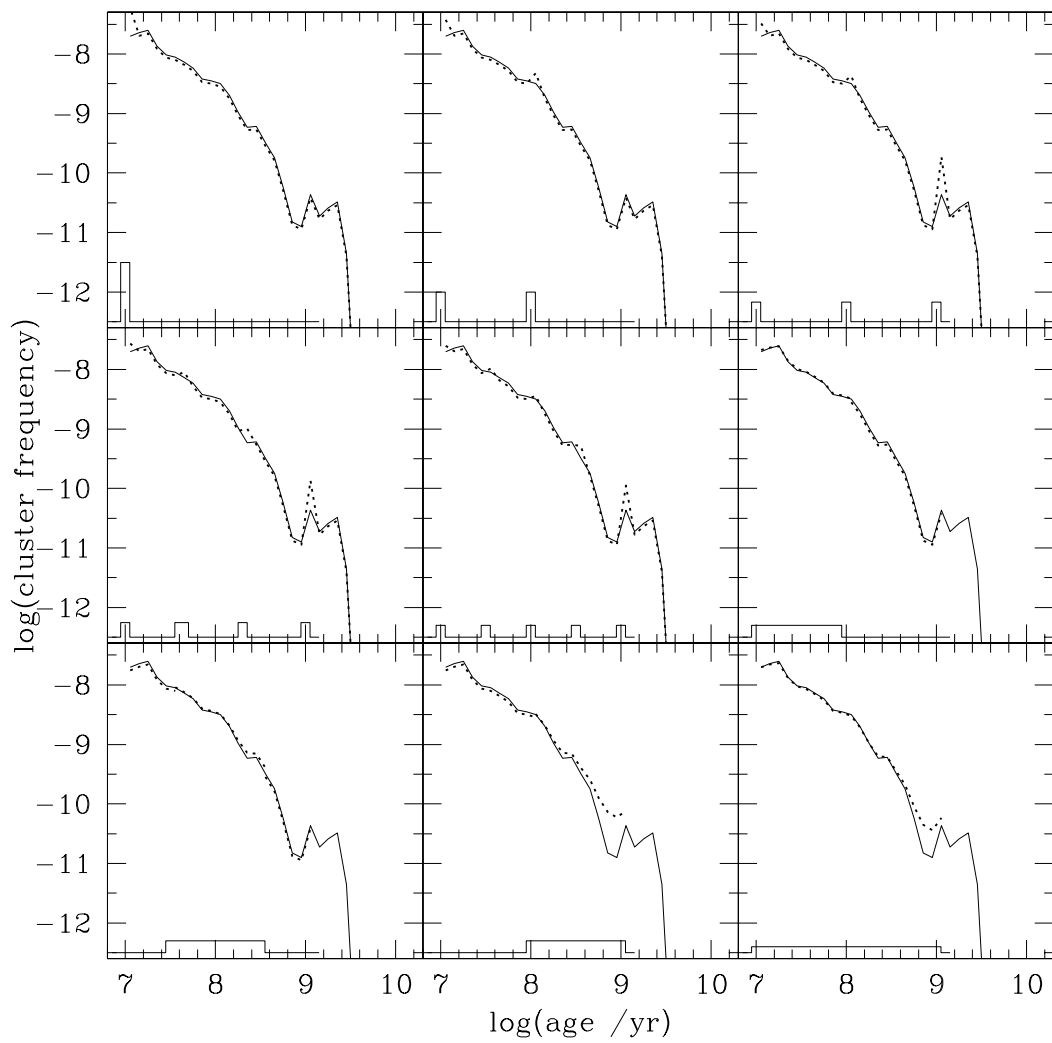


Figure A7. CFs for the 30 Doradus (see Appendix A for details).

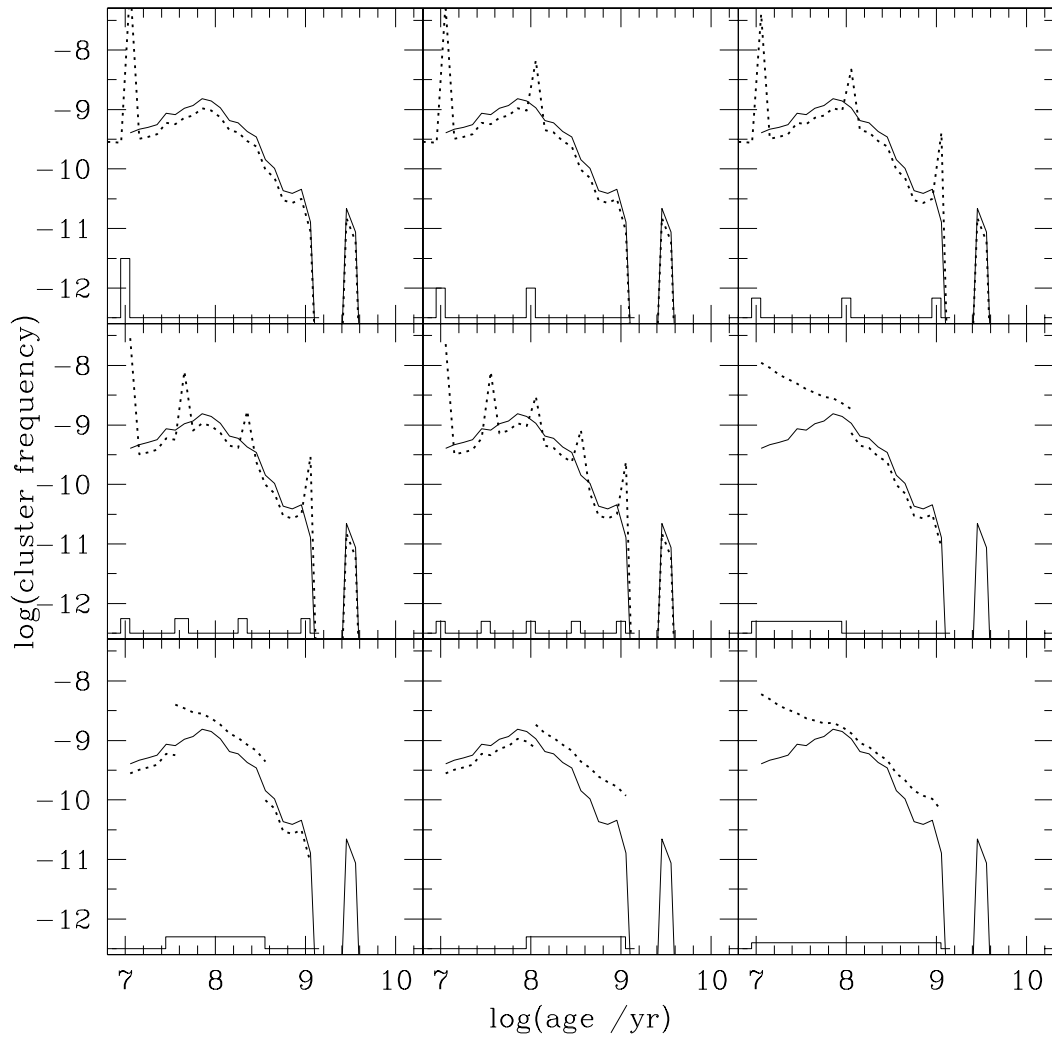


Figure A8. CFs for the LMC Southeast Arm (see Appendix A for details).